Anomalous increase in dielectric susceptibility during isothermal aging of ultrathin polymer films

Daisuke Tahara

Research Organization of Science and Engineering, Ritsumeikan University, Noji-Higashi 1-1-1, Kusatsu 525-8577, Japan

Koji Fukao*

Department of Physics, Ritsumeikan University, Noji-Higashi 1-1-1, Kusatsu 525-8577, Japan

The aging dynamics of poly(2-chlorostyrene) (P2CS) ultrathin films with thicknesses less than 10 nm were investigated using dielectric relaxation spectroscopy. The imaginary part of the dielectric susceptibility ϵ'' for P2CS ultrathin films with a thickness of 3.7 nm increased with an increase in isothermal aging time, while this was not the case for P2CS thin films thicker than 9.0 nm. This anomalous increase in ϵ'' for the ultrathin films is strongly correlated with the presence of a mobile liquidlike layer within the thin films.

I. INTRODUCTION

In the glassy state, the dynamical mode is completely frozen [1]. The dynamical mode is referred to as the α process and is commonly observed in liquid states above the glass transition temperature T_g. In polymeric systems, segmental motion is the microscopic origin of the α process [2]. However, even in the glassy state there is a very slow change in the structure and dynamics when approaching an equilibrium state, and this phenomenon is known as physical aging [3]. Several interesting phenomena, including memory and rejuvenation effects, occur during physical aging [3–5]. These effects are frequently observed in many disordered systems, including polymer glasses [6–11], spin glasses [12–15], and other disordered systems [16–18].

We have previously investigated the aging dynamics in polymer glasses of poly(methyl methacrylate) (PMMA) [8–10], polystyrene (PS) [19,20], and poly(2-chlorostyrene) (P2CS) [21] using dielectric relaxation spectroscopy and temperature modulated differential scanning calorimetry. In PMMA, the real and imaginary parts of dielectric susceptibility decrease with increasing aging time for isothermal aging. This result is consistent with the idea that the nonequilibrium glassy state approaches an equilibrium state. In PS and P2CS, we have successfully observed the simultaneous decrease in both the *dielectric susceptibility and volume* using single capacitance measurements. The memory and rejuvenation effects of the dielectric susceptibility characteristic of the aging dynamics have different behavior from that for volume.

On the other hand, recent research has shown that segmental motion, which is frozen in the glassy state, is strongly dependent on the film thickness [22,23]. T_g decreases with decreasing film thickness; and, accordingly, the dynamics of the α process, the segmental motion, becomes faster in thinner films [23–25]. It is very natural to expect that there is a characteristic thickness dependence of the aging dynamics in thin polymer films. There have been several reports on the dependence of the aging dynamics on thickness [8,26–29].

In this paper, we have investigated the aging dynamics of P2CS ultrathin films in order to elucidate the detailed aging dynamics. An interesting dependence of the time evolution of the dielectric susceptibility for isothermal aging on thickness has been observed from the dielectric measurements. The microscopic origin of the thickness dependence of the aging dynamics has been discussed on the basis of segmental dynamics measurements using dielectric relaxation spectroscopy.

In Sec. II of this paper, the experimental details are described. An anomalous increase in the dielectric susceptibility observed in ultrathin P2CS films during isothermal aging is reported in Sec. III, and observation of the segmental dynamics in ultrathin P2CS films is described in Sec. IV. In Secs. V and VI, the microscopic origin of the anomaly is discussed on the basis of the observed results. Finally, concluding remarks are given in Sec. VII.

II. EXPERIMENTS

P2CS was used as the polymer sample and was purchased from Polymer Source, Inc. (weight-averaged molecular weight $M_w = 3.3 \times 10^5$, $M_w/M_n = 2.2$). Thin films of P2CS were prepared by spin coating a P2CS/toluene solution on a glass substrate on which aluminum (Al) had been vacuum deposited. The film thickness was controlled by varying the concentration of the solution; P2CS thin films with thickness d of 3.7, 5.4, 9.0, 9.5, and 22 nm were prepared. After annealing at 343 K under vacuum for 2 days, Al was again vacuum deposited to serve as an upper electrode. In order to obtain reproducible results, several heating cycles up to and exceeding the bulk value of T_g were carried out prior to capacitance measurements of the relaxed as-spun films. The thickness dependence of T_g for single thin films of P2CS has been measured by using capacitance measurements [30]. The observed thickness dependence is given as follows:

$$T_g(d) = \begin{cases} \Delta T_g (d - d_c) + T_{g,c}: & d < d_c \\ T_{g,\infty} - \dfrac{d_c}{d}(T_{g,\infty} - T_{g,c}): & d > d_c, \end{cases} \quad (1)$$

where $\Delta T_g = 0.28 \pm 0.07$ K/nm, $d_c = 30 \pm 11$ nm, $T_{g,c} = 384.2 \pm 2.7$ K, and $T_{g,\infty} = 388.5 \pm 0.6$ K. From Eq. (1), the

---

*Corresponding author; fukao.koji@gmail.com
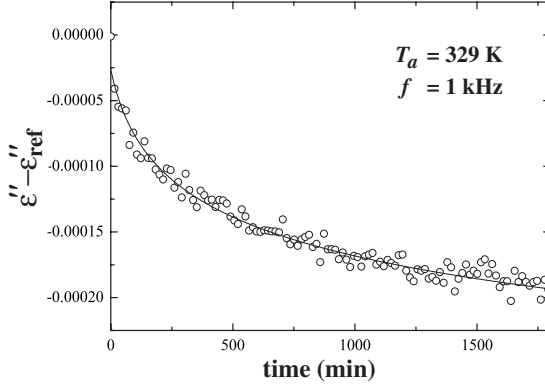
FIG. 1. Aging time dependence of $\epsilon'' - \epsilon''_{\text{ref}}$ for $d=22$ nm, $f=1$ kHz, and $T_a=329$ K. The solid line is fitted using Eq. (2), where $\Delta\epsilon = 0.0082$, $t_0 = 62$ min, and $n=0.07$.

values of T_g for thin films are 381.9, 378.4, 377.3, and 376.8 K for $d=22$, 9.5, 5.4, and 3.7 nm, respectively. The thickness of the as-prepared films was evaluated from electrical capacitance measured at 273 K, according to a previously reported procedure [23,24].

Capacitance measurements were carried out using an *LCR* meter (Agilent Technology, 4284A) for the frequency f range from 20 Hz to 1 MHz during cooling and heating between 425 and 273 K at a rate of 1 K/min, and during isothermal aging at various aging temperatures T_a (=300–357 K). The complex dielectric constant ϵ^* ($\equiv \epsilon' - i\epsilon''$) was evaluated as a function of temperature T and aging time t_w from the value of the complex electrical capacitance of the sample condenser C^* ($\equiv C' - iC''$), on the assumption that $C^* = \epsilon^* C_0$ is valid, where C_0 is the geometrical capacitance of the sample condenser.

The following two temperature protocols were employed:

(1) *Isothermal aging*: In this temperature protocol, the temperature was changed from a high temperature of 425 K (above T_g) to an aging temperature T_a (below T_g), and then the temperature was maintained at T_a for t_a hours.

(2) *Constant-rate mode*: The temperature was decreased from 425 to 273 K at a constant rate of 1 K/min, and then increased from 273 to 425 K at the same rate. This is a simple constant-rate mode, and we refer to this temperature change as the reference mode. In addition to the above thermal treatment, we included an intermittent stop at T_a for t_a hours during cooling from 425 to 273 K. This temperature protocol is denoted as $\mathcal{C}(T_a, t_a)$. According to this notation, the reference mode corresponds to the protocol $\mathcal{C}(T_a, 0)$ for any value of T_a.

III. AGING DYNAMICS IN ULTRATHIN P2CS FILMS

Figure 1 shows the aging time dependence of the dielectric loss ϵ'' relative to the value ϵ''_{ref} for P2CS thin films undergoing isothermal aging at $T_a=329$ K, where $\Delta T_a \equiv T_g - T_a = 52.9$ K. The value of ϵ''_{ref} is ϵ'' at $t_w=0$. This figure shows that ϵ'' decreases with increasing aging time. The system approaches an equilibrium state during isothermal aging, even in the glassy state, so that the dielectric
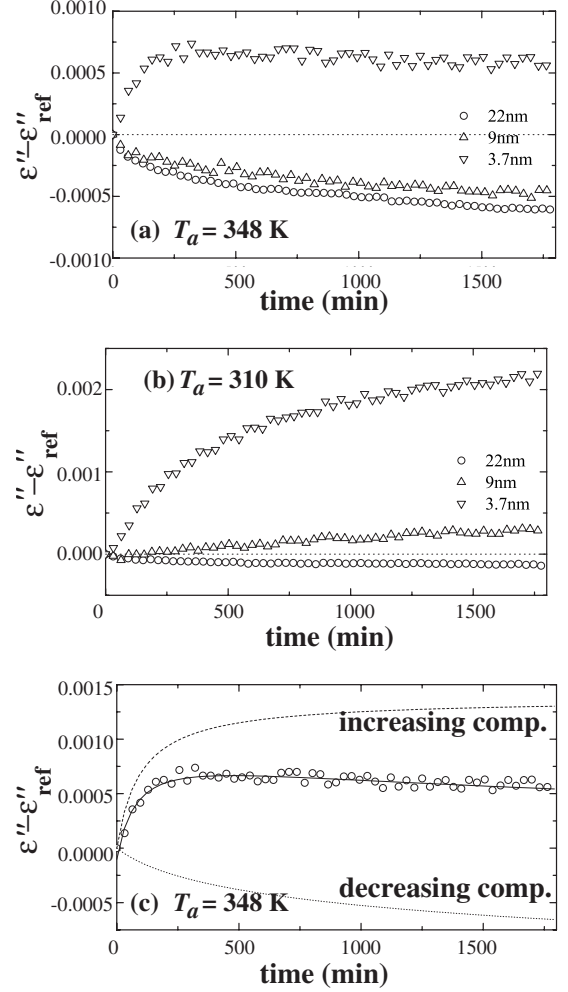
FIG. 2. Aging time dependence of $\epsilon'' - \epsilon''_{\text{ref}}$ for thin films with $d=22$, 9.0, and 3.7 nm and $f=200$ Hz. (a) $T_a=348$ K, (b) $T_a=310$ K, and (c) aging time dependence of $\epsilon'' - \epsilon''_{\text{ref}}$ for thin films with $d=3.7$ nm and $f=200$ Hz, in addition to both the increasing component ($\Delta\epsilon''_{\text{in}}$, dashed line) and decreasing component ($\Delta\epsilon''_{\text{dec}}$, dotted line).

constant changes slowly with aging time. The aging time t_w dependence of ϵ'' can be fitted to the equation

$$\epsilon''(t_w; f, T_a) = \frac{\Delta\epsilon}{\left(1 + \frac{t_w}{t_0}\right)^n} + \epsilon''(\infty; f, T_a), \quad (2)$$

where $\Delta\epsilon$ is the relaxation strength toward the equilibrium value, t_0 is the characteristic time of the aging dynamics, and n is an exponent [8]. This relation can be applied to relatively thick films. The t_w dependence for thinner films is different from this one and is discussed later.

Figure 2 shows the t_w dependence of ϵ'' for P2CS thin films of $d=22$, 9.0, and 3.7 nm and for two different aging temperatures T_a of 348 and 310 K. The frequency of the applied electric field was 200 Hz. In Fig. 2(a), the value of ϵ'' decreases with increasing aging time at $T_a=348$ K, except for the initial stage of thin films with $d=3.7$ nm. However, the value of ϵ'' clearly increases for isothermal aging at $T_a=310$ K in the P2CS thin films with $d=3.7$ and 9.0 nm.
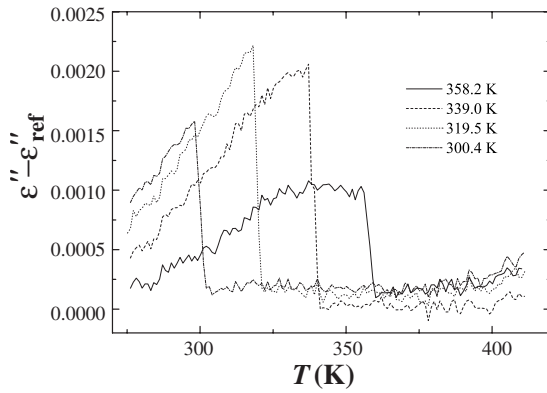
FIG. 3. Temperature dependence of the ϵ'' deviation from the reference values for $d=3.7$ nm observed during cooling, including isothermal aging at various T_a.

These results suggest that the t_w dependence of ϵ'' is strongly dependent on the thickness and aging temperature. For thin films with $d=3.7$ nm, ϵ'' monotonically increases with increasing aging time at a lower aging temperature T_a (=310 K), while ϵ'' shows a maximum against the aging time for $T_a=348$ K. The latter result suggests that *there are two competing physical origins with different time scales.* Figure 2(c) shows how the aging time dependence of $\epsilon''-\epsilon''_{ref}$ at isothermal aging at $T_a=348$ K for $d=3.7$ nm can be decomposed into two competing, increasing and decreasing, components. Results of the detailed analyses are shown in Sec. V.

Figure 3 shows the temperature dependence of the imaginary part of the dielectric constant ϵ'' relative to the reference value ϵ''_{ref} for the cooling process, including isothermal aging for 30 h. Here, the values of $\epsilon''_{ref}(f,T)$ have been measured during the heating and cooling processes at a rate of 1 K/min without any isothermal aging, i.e., the protocol $\mathcal{C}(T_a,0)$. For each temperature, the deviation $\epsilon''(f,T)-\epsilon''_{ref}(f,T)$ was evaluated. Figure 3 shows that ϵ'' increases with increasing aging time t_w for isothermal aging at various aging temperatures T_a, as shown in Fig. 2. The deviation of ϵ'' from ϵ''_{ref} induced during the isothermal aging decreases with decreasing temperature for the subsequent cooling and ϵ'' approaches ϵ''_{ref}. This temperature dependence shows that there is a *rejuvenation effect*, as reported for the glassy state in PMMA [6,8]. Figure 3 shows that the amount of increase in ϵ'' induced during isothermal aging for 30 h is not a monotonic function of the aging temperature T_a, but has a maximum at $T_a=320$ K. The aging temperature dependence of the amount of deviation for ultrathin P2CS films is completely different from that for PMMA [6,8], and also for thicker films of P2CS [21]. If there is only one dynamical mode associated with the aging phenomena, then the amount of deviation should be a monotonic function of the annealing temperature. Therefore, this annealing temperature dependence also suggests that there are *two competing processes* that have different temperature dependences.

IV. SEGMENTAL DYNAMICS IN ULTRATHIN P2CS FILMS

As discussed in Sec. III, the aging dynamics of ultrathin P2CS films are quite different from those of thicker films and
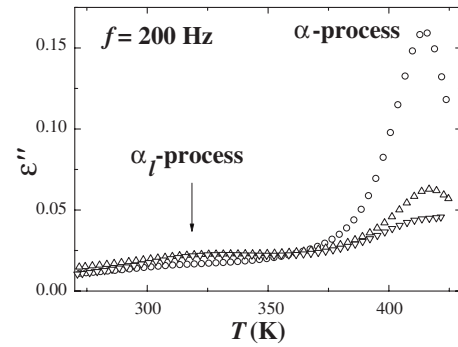
FIG. 4. Temperature dependence of the imaginary part of the complex dielectric constant ϵ'' for $d=9.5$ ($\bigcirc$), 5.4 ($\triangle$), and 3.7 ($\bigtriangledown$) nm. The data points in this figure were obtained for the cooling process at $f=200$ Hz.

have an anomalous dependence on the thickness and temperature. Here, the microscopic origin for such an anomaly is discussed on the basis of segmental dynamics measurements using dielectric relaxation spectroscopy.

In previous studies on PS thin films, the glass transition temperature T_g decreased with decreasing film thickness, and the amount of decrease in T_g was approximately 20 K when the film thickness was decreased from the bulk value to 10 nm [22]. Accordingly, the dynamics of the α process become faster in thinner films [23]. There are several physical reasons for the decrease in T_g, and the increase in the relaxation rate of the α process. One is the existence of a liquidlike layer with higher mobility near the free surface [31,32]. Furthermore, the distribution of T_g within thin films is also important for the overall dynamics in thin polymer films [33–35].

Figure 4 shows the temperature dependence of ϵ'' for the P2CS thin films with $d=9.5$, 5.4, and 3.7 nm at 200 Hz. There is a loss peak due to the α process around 415 K, and the peak height decreases with decreasing film thickness. In addition to this behavior, another process around 320 K is evident only for the $d=3.7$ nm thin film. This peak of ϵ'' due to another process is also observed for thin films of both PS and PS labeled with a dye (DR1; disperse red one) [23,36]. This extra loss peak was attributed to the segmental motion of a liquidlike layer near the surface or interface, which we have labeled as the α_l process. The loss peak observed for ultrathin P2CS films may also be attributed to the α_l process. If the thickness of the liquidlike layer is independent of the overall thickness, then the contribution of the liquidlike layer becomes more appreciable as the thickness decreases. Figure 4 shows that the dielectric loss peak due to the α process is reduced; and, accordingly, that of the α_l process becomes more appreciable as the film thickness is decreased to $d=3.7$ nm.

Figure 5 shows the temperature dependence of ϵ'' for $d=5.4$ nm obtained at three different frequencies of $f=20$ Hz, 200 Hz, and 2 kHz. The peak due to the α_l process is shifted to the higher temperature side as f is changed to higher frequency, which suggests that the loss peak around 300 K, the α_l process, has dynamical character. In order to analyze the observed dielectric loss, it is assumed that there are three contributions, such as the α process, α_l process, and
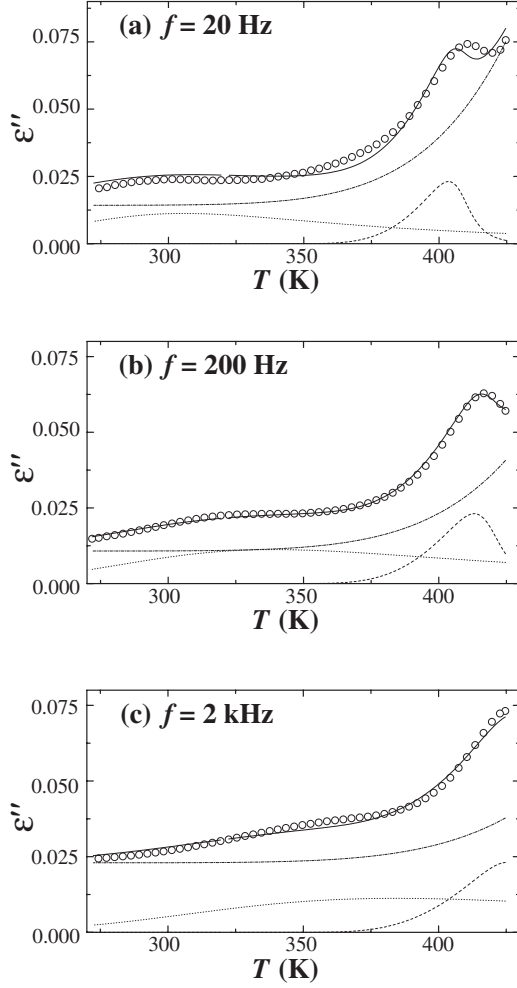
FIG. 5. Temperature dependence of the imaginary part of the complex dielectric constant ϵ'' for $d=5.4$ nm obtained at $f=$ (a) 20 Hz, (b) 200 Hz, and (c) 2 kHz. The solid line is calculated using Eq. (3) with the best-fit parameters. The dashed, dotted, and dashed-dotted lines correspond to the components of the α process, the α_l process, and the conductivity, respectively.

conductivity components. Therefore, we describe the complex dielectric constant ϵ^* as follows:

$$\epsilon^*(f,T) = \sum_{i=\alpha,\alpha_l} \frac{\Delta\epsilon_i}{[1+(i2\pi f\tau_i)^{\alpha_i}]^{\beta_i}} + i\frac{\sigma}{\epsilon_0(2\pi f)^m}, \quad (3)$$

where the first terms on the right-hand side are contributions from the α and α_l processes, as described by the Havriliak-Negami (HN) equations [37], $\Delta\epsilon_i$ is the dielectric strength of the i process, α_i and β_i are the shape parameters, and τ_i is the relaxation time. τ_i can be described by the Vogel-Fulcher-Tammann (VFT) equation [38]

$$\tau_i(T) = \tau_{0,i}\exp\left(\frac{T_{A,i}}{T-T_{V,i}}\right), \quad (4)$$

where $\tau_{0,i}$, $T_{A,i}$, and $T_{V,i}$ are constants. The second term on the right-hand side of Eq. (3) is the contribution from the conductivity component, where m is an exponent, ϵ_0 is the dielectric permittivity *in vacuo*, and σ is the conductivity. This conductivity component becomes more important as the thickness decreases. The conductivity σ can be described by using a VFT-like equation,

$$\sigma(T) = \frac{A}{T^{0.5}}\exp\left(\frac{T_{A,c}}{T-T_{V,c}}\right), \quad (5)$$

where A, $T_{A,c}$, and $T_{V,c}$ are constants [39]. The temperature dependence of ϵ'' can be fitted using Eq. (3) in addition to the constant background intensity. The solid curve in Fig. 5 is the curve calculated for ϵ'' using the best-fit parameters listed in Table I. Each component in Eq. (3) is also shown as the dashed, dotted, and dashed-dotted lines in Fig. 5. The fitting parameters listed in Table I are commonly obtained for the three different frequencies $f=20$ Hz, 200 Hz, and 2 kHz. For the fitting procedures, the parameters of T_A and T_V are assumed to be common for both the α_l process and the conductivity component.

TABLE I. Best-fit parameters for the frequency and temperature dependence of the dielectric loss ϵ'' observed for the P2CS ultrathin films with $d=9.5$, 5.4, and 3.7 nm.

Process	d (nm)	α_i	β_i	$\tau_{0,i}$ (s)	$T_{A,i}$ (K)	$T_{V,i}$ (K)	$\Delta\epsilon_i$
α	9.5	0.68 ± 0.04	0.38 ± 0.03	$(1.8\pm0.2)\times10^{-12}$	1892 ± 1	324.6 ± 0.1	0.65 ± 0.03
	5.4	0.95 ± 0.11	0.22 ± 0.04	$(5.4\pm1.0)\times10^{-12}$	1884.4 ± 0.9	319.6 ± 0.1	0.12 ± 0.02
	3.7	0.65 ± 0.20	0.21 ± 0.11	$(1.3\pm1.0)\times10^{-11}$	1750.5 ± 0.8	317.2 ± 0.1	0.075 ± 0.030
α_l	9.5	0.26	1	3.5×10^{-8}	4.3×10^3	61	0.26 ± 0.13
	5.4	0.36 ± 0.12	1	$(1.1\pm4.8)\times10^{-10}$	$(4.2\pm2.6)\times10^3$	75 ± 92	0.078 ± 0.014
	3.7	0.42 ± 0.09	1	$(0.87\pm2.6)\times10^{-10}$	$(4.2\pm1.5)\times10^3$	72 ± 45	0.107 ± 0.010

Process	d (nm)	A	m	$T_{A,c}$ (K)	$T_{V,c}$ (K)
	9.5	2.0×10^{-5}	0.58 ± 0.24	4.3×10^3	61
Conductivity comp.	5.4	7.4×10^{-6}	0.31 ± 0.04	$(4.2\pm2.6)\times10^3$	75 ± 92
	3.7	$(1.1\pm3.2)\times10^{-5}$	0.34 ± 0.04	$(4.2\pm1.5)\times10^3$	72 ± 45
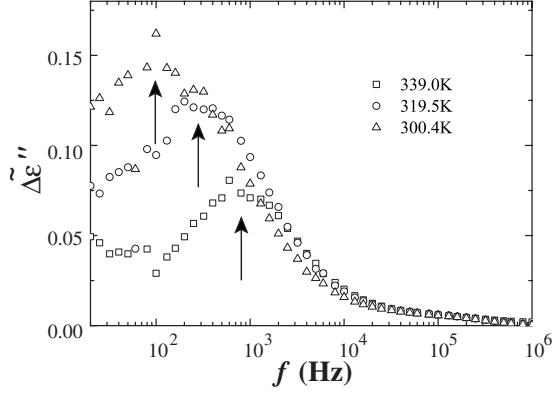
FIG. 6. Frequency dependence of $\Delta\tilde{\epsilon}''$ after isothermal aging at three different aging temperatures T_a=339.0 (□), 319.5 (○), and 300.4 (△) K for 30 h with d=3.7 nm.

V. MICROSCOPIC ORIGIN OF THE ANOMALY

Here, we return to the aging dynamics that could be observed for isothermal aging at T_a. For a given frequency f, we could observe the change in $\epsilon''(t_\omega;f,T_a)$ from $\epsilon''_{\rm ref}$ [$\equiv\epsilon''(t_\omega=0;f,T_a)$] (before isothermal aging at temperature T_a) to $\epsilon''(t_\omega=30 \ h;f,T_a)$ after isothermal aging for 30 h. Here, we define the relative relaxation strength due to the isothermal aging as

$$\Delta\tilde{\epsilon}'(f,T_a) \equiv \frac{\epsilon''(t_w=30 \ h;f,T_a) - \epsilon''(t_w=0;f,T_a)}{\epsilon''(t_w=0;f,T_a)}. \quad (6)$$

Figure 6 shows that the relative relaxation strength $\Delta\tilde{\epsilon}'$ has a peak against frequency, and the peak frequency $f_{\max}$ is strongly dependent on the aging temperature T_a. The frequency dependence of $\Delta\tilde{\epsilon}'$ suggests that *there may be a relation between the aging dynamics and a dynamical mode with a characteristic time* ($\sim 1/f_{\max}$). It has been previously reported that for PMMA thin films, the relaxation strength for structural change during isothermal aging becomes larger with decreasing frequency at a given aging temperature and does not show a peak at any frequency [6,8]. The frequency dependence of the relaxation strength due to isothermal aging for ultrathin P2CS films is completely different from that for PMMA.

A distinct peak of $\Delta\tilde{\epsilon}''$ in the frequency domain at a given aging temperature was observed in Fig. 6. A similar behavior related to the α_l process could also be observed in the temperature domain at a given frequency. As already shown in Fig. 2, there are two competing processes that have different aging times and temperature dependences for isothermal aging at T_a. Here, we consider the time evolution of the dielectric loss ϵ'' for isothermal aging at T_a. For this process, it is assumed that there are two components: $\Delta\epsilon''_{\rm in}$ is the component that increases with aging time, and $\Delta\epsilon''_{\rm dec}$ is the component that decreases with aging time:

$$\epsilon''(t_\omega;f,T_a) - \epsilon''_{\rm ref} = \Delta\epsilon''_{\rm in}(t_\omega;f,T_a) + \Delta\epsilon''_{\rm dec}(t_\omega;f,T_a), \quad (7)$$

where

$$\epsilon''_{\rm ref} \equiv \epsilon''(t_\omega=0;f,T_a), \quad (8)$$

$$\Delta\epsilon''_{\rm in}(t_\omega;f,T_a) \equiv \Delta\epsilon_l\left[1 - \left(1 + \frac{t_\omega}{t_l}\right)^{-n_l}\right], \quad (9)$$

$$\Delta\epsilon''_{\rm dec}(t_\omega;f,T_a) \equiv \Delta\epsilon_b\left[\left(1 + \frac{t_\omega}{t_b}\right)^{-n_b} - 1\right]. \quad (10)$$

The values t_l and t_b are the characteristic times, n_l and n_b are the exponents, and $\Delta\epsilon_l$ and $\Delta\epsilon_b$ are the relaxation strengths for the increasing and decreasing components, respectively. Here, we have decomposed the time evolution of $\epsilon''-\epsilon''_{\rm ref}$ into two competing components, $\Delta\epsilon''_{\rm in}$ and $\Delta\epsilon''_{\rm dec}$, using Eqs. (9) and (10) for isothermal aging at T_a and three different frequencies for ultrathin P2CS films with d=3.7 nm. The best-fit parameters for the time evolution of $\epsilon''-\epsilon''_{\rm ref}$ for isothermal aging at T_a are listed in Table II. For the fitting procedures, the parameter n_l is fixed to 1 and the parameters t_b and n_b for fitting the data for d=3.7 nm are fixed to those obtained by fitting the observed data to Eq. (10) with 2 and 4 kHz for d=22 nm. For the decreasing component $\Delta\epsilon''_{\rm dec}$, only the value of $\Delta\epsilon_b$ is adjusted in order to reproduce the observed results for d=3.7 nm at the three different frequencies. An example of the decomposition of ϵ'' into $\Delta\epsilon''_{\rm in}$ and $\Delta\epsilon''_{\rm dec}$ is shown in Fig. 2(c).

From the decomposition procedures, we have obtained the relaxation strength $\Delta\epsilon_l$ of the increasing components as a function of the aging temperature T_a for given frequencies of

TABLE II. Best-fit parameters for the aging time dependence of $\epsilon''-\epsilon''_{\rm ref}$ for isothermal aging at T_a=300−358 K and for f=2 kHz, 200 Hz, and 20 Hz.

| T_a (K) | f=2 kHz | | | f=200 Hz | | | f=20 Hz | | | | |
	$\Delta\epsilon_l$	t_l(min)	$\Delta\epsilon_b$	$\Delta\epsilon_l$	t_l(min)	$\Delta\epsilon_b$	$\Delta\epsilon_l$	t_l(min)	$\Delta\epsilon_b$	t_b(min)	n_b
358.2	0.00183	102 ± 1	0.00558	0.00085	61 ± 3	0.00349	0.00153	68 ± 2	0.00741	45 ± 1	0.036 ± 0.003
348.6	0.00247	165 ± 2	0.00603	0.00137	97 ± 3	0.00636	0.00198	122 ± 3	0.01046	157 ± 3	0.043 ± 0.005
339.2	0.00300	233 ± 2	0.00839	0.00275	178 ± 4	0.01969	0.00275	153 ± 2	0.02216	120 ± 6	0.026 ± 0.009
329.4	0.00278	324 ± 2	0.00483	0.00396	250 ± 3	0.03159	0.00402	199 ± 2	0.04524	76 ± 4	0.017 ± 0.011
319.5	0.00232	402 ± 2	0	0.00387	413 ± 9	0.02705	0.00491	391 ± 5	0.07393	317 ± 12	0.018 ± 0.009
310.1	0.00202	450 ± 2	0	0.00329	471 ± 5	0.01145	0.00533	418 ± 3	0.06581	113 ± 12	0.010 ± 0.020
300.4	0.00189	634 ± 5	0	0.00272	632 ± 6	0	0.00472	614 ± 5	0.05685	220 ± 30	0.010 ± 0.040
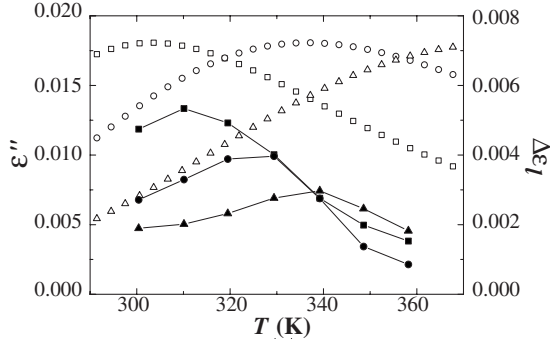
FIG. 7. Temperature dependence of the α_l-process component of ϵ'' at $f=20$ Hz ($\square$), 200 Hz ($\bigcirc$), and 2 kHz ($\triangle$) and aging temperature dependence of the increasing ϵ'' component during isothermal aging, $\Delta\epsilon_l$ at $f=20$ Hz ($\blacksquare$), 200 Hz ($\bullet$), and 2 kHz ($\blacktriangle$).

$f=20$ Hz, 200 Hz, and 2 kHz (see the full symbols in Fig. 7). In order to compare the aging dynamics with the dynamical mode of the α_l process, we also plotted the component of ϵ'' in Fig. 7, only for the α_l process that has been reproduced using the HN equation with the best-fit parameters for the α_l process listed in Table I (see the open symbols in Fig. 7). Figure 7 shows that the temperature dependence of the aging strength due to the increasing component is strongly associated with that of the dielectric loss due only to the α_l process.

Figure 8 shows Arrhenius plots of the relaxation times for the α and α_l processes obtained by the peak frequency of the dielectric loss ϵ'' for P2CS thin films with $d=3.7$ nm. The peak frequencies $f_{\max,\alpha}$ and $f_{\max,\alpha_l}$ are evaluated from the frequency dependence of the dielectric loss due only to the α and α_l processes that are reproduced from Eq. (3) with best-fit parameters. The peak frequency of $\Delta\tilde{\epsilon}''(f,T_a)$ after isothermal aging at a given aging temperature T_a for 30 h and with $d=3.7$ nm is also plotted in Fig. 8. The peak frequency is evaluated from the observed frequency dependence of $\Delta\tilde{\epsilon}''$ in Fig. 6.

From Fig. 8, the temperature dependence of the characteristic time τ evaluated from the aging dynamics ($\triangle$) is quite similar to that evaluated from the dynamics of the α_l
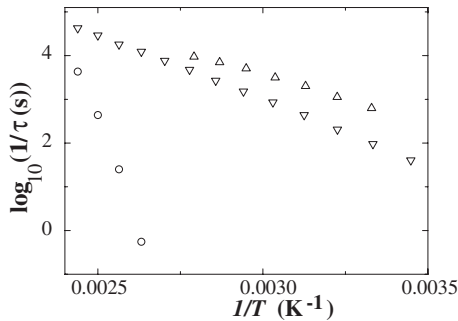
FIG. 8. Arrhenius plots for the α and α_l processes of ultrathin P2CS films with $d=3.7$ nm. The value of τ is evaluated from the relationship $\tau=1/2\pi f_{\max}$. The symbol $\bigcirc$ corresponds to the data obtained from the peak frequency $f_{\max}$ of the dielectric loss ϵ'' due only to the α process, which is evaluated by fitting the observed values of ϵ'' to Eq. (3). The symbol $\triangledown$ corresponds to the data due only to the α_l process. The symbol $\triangle$ corresponds to the peak frequency of $\Delta\tilde{\epsilon}''$ in Fig. 6 at a given aging temperature T_a.
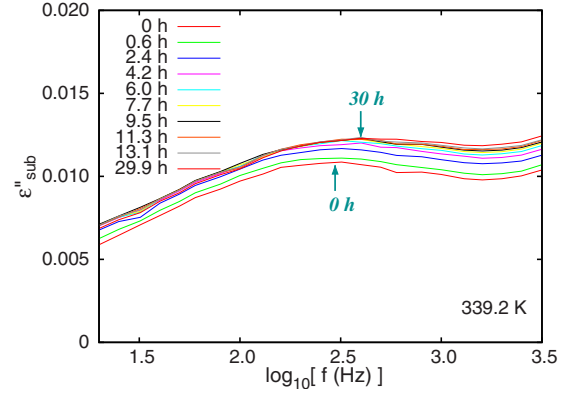
FIG. 9. (Color online) The dependence of the dielectric loss ϵ''_{sub} on the logarithm of the frequency f observed for the isothermal aging at $T_a=339.2$ K for the thin films of P2CS with $d=3.7$ nm. The lowest and highest curves are the results at $t_w=0$ and 30.0 h, respectively. The value $\epsilon''_{\text{sub}}(t_w;f,T_a)$ for the isothermal aging is evaluated by subtracting the value observed at 273.0 K observed during the cooling process at the rate of 1 K/min from the value $\epsilon''(t_w;f,T_a)$.

process ($\triangledown$), but is completely different from that evaluated from the dynamics of the α process ($\bigcirc$). Therefore, it can be concluded that the anomalous increase in dielectric susceptibility observed for isothermal aging of ultrathin P2CS films is strongly associated with the α_l process.

VI. CHANGE IN THE α_l PROCESS DURING ISOTHERMAL AGING

Here, the evolution of the dielectric loss of the α_l process during the isothermal aging is discussed. As shown in the previous section, the dielectric loss ϵ'' increases with increasing aging time for the isothermal aging for ultrathin films of P2CS with a thickness of 3.7 nm. The increase in ϵ'' observed for the isothermal aging may be associated with the occurrence of the α_l process for the ultrathin films of P2CS.

Figure 9 shows the aging time dependence of the dielectric loss as a function of the logarithm of the frequency during the isothermal aging at $T_a=339.2$ K for ultrathin films of P2CS with $d=3.7$ nm. The dielectric loss ϵ'' shown in Fig. 9 is the value obtained after subtraction of the values observed at 273 K. In Fig. 9, the dielectric loss peak due to the α_l process is clearly shifted to the higher frequency side, and at the same time the peak height increases with increasing aging time during the isothermal aging process. In order to obtain the dependence of the dielectric loss of the α_l process on the aging time more in detail, we have extracted the peak frequency and the peak height of the α_l process as functions of the aging time t_w for the isothermal aging at T_a.

Figure 10 clearly shows that both the peak frequency and the peak height of the α_l process increase with aging time. Furthermore, we notice that the increasing rate of the peak frequency and the peak height decreases with increasing aging time. Therefore, it can be concluded that the anomalous increase in ϵ'' observed for the ultrathin films of P2CS with $d=3.7$ nm is associated with the increase in both the peak
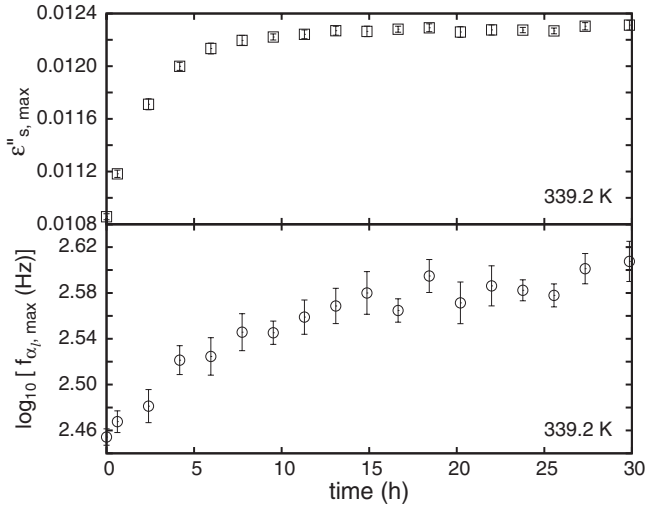
FIG. 10. The aging time dependence of the dielectric loss maximum $\epsilon''_{s,\max}$ and the maximum frequency $f_{\alpha_l,\max}$ of the α_l process evaluated from the dielectric spectra in Fig. 9.

TABLE III. Relative decrease in volume for isothermal aging at T_a for 30 h; $\Delta\widetilde{v} \equiv -[v(t_\omega=30 \text{ h})-v(t_\omega=0)]/v(t_\omega=0)$, where $v(t_\omega)$ is the volume at time t_ω, the maximum relative deviation of C'' from the initial value at $t_\omega=0$ during isothermal aging; $\Delta\widetilde{C}'' \equiv [C''(t_\omega=t_{\max})-C''(t_\omega=0)]/C''(t_\omega=0)$, where $C''(t_\omega)$ is the imaginary part of the complex electric capacitance at t_ω for an applied electric field frequency of $f=1$ kHz, and $t_{\max}$ is the time at which C'' has a maximum during isothermal aging; and the ratio between $\Delta\widetilde{C}''$ and $\Delta\widetilde{v}$.

T_a (K)	$\Delta\widetilde{v}$	$\Delta\widetilde{C}''$	$\Delta\widetilde{C}''/\Delta\widetilde{v}$
300	0.114	8.44×10^{-2}	74.1
319	0.136	9.93×10^{-2}	73.0
339	0.159	7.44×10^{-2}	46.7
358	0.230	2.90×10^{-2}	12.6

frequency and the peak height of the dielectric loss due to the α_l process for the isothermal aging.

VII. CONCLUDING REMARKS

The occurrence of the α_l process may lead to the increase in the dielectric susceptibility with isothermal aging. The most probable candidate for the microscopic origin of the α_l process is the presence of a mobile interfacial region where the polymer chains can maintain their mobility, even below the bulk T_g. Such mobility can destroy the "ordering" that is developed during the aging process. In other words, the mobility can rejuvenate the glassy state for ultrathin films of P2CS.

The present measurements showed that the dielectric susceptibility increases with increasing aging time for the isothermal aging of ultrathin P2CS films. Here, we have a question on how the mobile layer can increase the dielectric susceptibility with increasing aging time. For thin polymer films, de Gennes proposed that there is a sliding motion for the thin-film geometry of polymers [40,41]. Even in the glassy state, a polymer chain can move along its own contour if there is an interfacial mobile layer.

The occurrence of the sliding motion can cause polymer chains in the bulk region to move to the mobile region near the interface during isothermal aging. The number of polymer chains that belong to the mobile region increases, and the fraction of polymer chains that contribute to the α_l process increases. This phenomenon manifests as an increase in

ϵ'' for isothermal aging at a given temperature and frequency. We propose this as a possible scenario for the present anomalous increase in ϵ'' for isothermal aging.

Our previous measurements of P2CS thin films with thicknesses greater than 10 nm showed that both the dielectric susceptibility and volume decrease with an increase in the aging time for isothermal aging [21]. The decrease in volume causes an increase in the electric capacitance. In this case, the decrease in dielectric susceptibility competes with the decrease in volume for the determination of the aging time dependence of the electric capacitance. Therefore, we consider the possibility that the volume change during isothermal aging could cause an artificial increase in the dielectric susceptibility. Table III shows the decrease in volume and the increase in the imaginary part of the electric capacitance C'' for isothermal aging at $T_a=300-358$ K. The increment in C'' is far greater than the decrease in volume; therefore, the possibility of an artificial increase is denied. In summary, we have observed an anomalous increase in the dielectric susceptibility for the isothermal aging of ultrathin P2CS films below T_g, and the fraction of the interfacial mobile region where the polymer chains are mobile as observed in a liquid state can increase in accordance with the increase in dielectric susceptibility.

[1] J. Mark *et al.*, *Physical Properties of Polymers*, 3rd ed. (Cambridge University Press, Cambridge, England, 2003), Chap. 2.

[2] G. Strobl, *The Physics of Polymers* (Springer-Verlag, Berlin, 1996).

[3] L. C. Struick, *Physical Aging in Amorphous Polymers and Other Materials* (Elsevier, New York, 1978).

[4] A. J. Kovacs, J. J. Aklonis, J. M. Hutchinson, and A. A. Ramos, J. Polym. Sci., Polym. Phys. Ed. **17**, 1097 (1979).

[5] J.-P. Bouchaud, in *Soft and Fragile Matter*, edited by M. E. Cates and M. R. Evans (IOP Publishing, London, 2000), p. 185.

[6] L. Bellon, S. Ciliberto, and C. Laroche, Eur. Phys. J. B **25**, 223 (2002).

[7] L. Bellon, S. Ciliberto, and C. Laroche, e-print arXiv:cond-mat/9905160.

[8] K. Fukao and A. Sakamoto, Phys. Rev. E **71**, 041803 (2005).

[9] K. Fukao, A. Sakamoto, Y. Kubota, and Y. Saruyama, J. Non-Cryst. Solids **351**, 2678 (2005).

[10] K. Fukao and S. Yamawaki, Phys. Rev. E **76**, 021507 (2007).

[11] H. Bodiguel, F. Lequeux, and H. Montes, J. Stat. Mech.: Theory Exp. 2008, P01020.

[12] F. Lefloch, J. Hammann, M. Ocio, and E. Vincent, EPL **18**, 647 (1992).

[13] E. Vincent, J.-P. Bouchaud, J. Hamman, and F. Lefloch, Philos. Mag. B **71**, 489 (1995).

[14] K. Jonason, E. Vincent, J. Hammann, J.-P. Bouchaud, and P. Nordblad, Phys. Rev. Lett. **81**, 3243 (1998).

[15] K. Jonason, P. Nordblad, E. Vincent, J. Hammann, and J.-P. Bouchaud, Eur. Phys. J. B **13**, 99 (2000).

[16] P. Doussineau, T. de Lacerda-Aroso, and A. Levelut, EPL **46**, 401 (1999).

[17] R. L. Leheny and S. R. Nagel, Phys. Rev. B **57**, 5154 (1998).

[18] O. Kircher and R. Böhmer, Eur. Phys. J. B **26**, 329 (2002).

[19] K. Fukao and H. Koizumi, Eur. Phys. J. Spec. Top. **141**, 199 (2007).

[20] K. Fukao and H. Koizumi, Phys. Rev. E **77**, 021503 (2008).

[21] K. Fukao and D. Tahara, Phys. Rev. E **80**, 051802 (2009).

[22] J. Keddie, R. A. L. Jones, and R. A. Cory, EPL **27**, 59 (1994).

[23] K. Fukao and Y. Miyamoto, Phys. Rev. E **61**, 1743 (2000).

[24] K. Fukao, S. Uno, Y. Miyamoto, A. Hoshino, and H. Miyaji, Phys. Rev. E **64**, 051807 (2001).

[25] K. Fukao, Nihon Reoroji Gakkaishi **36**, 73 (2008).

[26] S. Kawana and R. A. L. Jones, Eur. Phys. J. E **10**, 223 (2003).

[27] C. J. Ellison, S. D. Kim, D. B. Hall, and J. M. Torkelson, Eur. Phys. J. E **8**, 155 (2002).

[28] R. D. Priestley, C. J. Ellison, L. J. Broadbelt, and J. M. Torkelson, Science **309**, 456 (2005).

[29] R. D. Priestley, L. J. Broadbelt, and J. M. Torkelson, Macromolecules **38**, 654 (2005).

[30] K. Fukao, Y. Oda, K. Nakamura, and D. Tahara, Eur. Phys. J. Spec. Top. (to be published).

[31] T. Kajiyama, K. Tanaka, I. Ohki, S.-R. Ge, S. J. Yoon, and A. Takahara, Macromolecules **27**, 7932 (1994).

[32] K. Akabori, K. Tanaka, T. Nagamura, A. Takahara, and T. Kajiyama, Macromolecules **38**, 9735 (2005).

[33] T. Kanaya, R. Inoue, K. Kawashima, T. Miyazaki, I. Tsukushi, T. Shibata, G. Matsuba, K. Nishida, and M. Hino, J. Phys. Soc. Jpn. **78**, 041004 (2009).

[34] K. Kawashima, R. Inoue, T. Kanaya, G. Matsuba, K. Nishida, and M. Hino, J. Phys.: Conf. Ser. **184**, 012004 (2009).

[35] C. J. Ellison and J. M. Torkelson, Nature Mater. **2**, 695 (2003).

[36] R. D. Priestley, L. J. Broadbelt, J. M. Torkelson, and K. Fukao, Phys. Rev. E **75**, 061806 (2007).

[37] S. Havriliak and S. Negami, Polymer **8**, 161 (1967).

[38] H. Vogel, Phys. Z. **22**, 645 (1921); G. S. Fulcher, J. Am. Ceram. Soc. **8**, 339 (1925).

[39] P. Jeevanandam and S. Vasudevan, J. Phys. Chem. B **102**, 4753 (1998).

[40] P. G. de Gennes, Eur. Phys. J. E **2**, 201 (2000).

[41] P. G. de Gennes, C. R. Acad. Sci., Ser IV: Phys., Astrophys. **1**, 1179 (2000).